Supporting Information

pH-Dependent Inversion of Hofmeister Trends in the Water Structure of the Electrical Double Layer

Emma L. DeWalt-Kerian[†], Sun Kim[†], Md. Shafiul Azam[‡], Hongbo Zeng[§], Qingxia Liu[§], Julianne M. Gibbs[†]*

[†]University of Alberta, Department of Chemistry, 11227 Saskatchewan Drive, Edmonton, Canada

‡ Bangladesh University of Engineering and Technology (BUET), Department of Chemistry, Dhaka, Bangladesh

§ University of Alberta, Department of Chemical and Materials Engineering, 11227 Saskatchewan Drive, Edmonton, Canada

* julianne.gibbs@ualberta.ca

I. Experimental Methods:

SFG Instrumentation. The laser system used in this study consists of a regeneratively amplified laser (Spitfire Pro, Spectra Physics, 1 kHz, 100 fs, 3.5 W) that is seeded and pumped by a femtosecond Ti:Sapphire oscillator (Spectra Physics, Mai Tai, 80 MHz) and a Nd:YLF laser (Spectra Physics, Empower), respectively. Two-thirds of the output light of the Spitfire (2.3 W) was used to pump a TOPAS-C optical parametric amplifier (OPA) (Light Conversion). The resulting broadband infrared light (FWHM ~130 nm) was tuned by using an nDFG OPA in the range of 2750 – 3300 nm to probe the broad O-H stretching modes of the interfacial water molecules. The light from the Spitfire (100 fs, λ = 800 nm) was stretched to a ps pulse using a Fabry-perot etalon (FWHM ~ 10 cm^{-1}) to generate a narrowband pulse (FWHM < 1 nm). The fs IR light (~20-25 μJ/pulse) and the ps visible light (~10 μJ /pulse) were focused onto the fused silica/water interface at angles of 64° and 60°, respectively, from surface normal. A tunable zero-order half-wave plate (Alphalas) was used to control the polarization of the IR light and a zero-

order 800 nm half-wave plate was used to control the polarization of the visible light. These two beams were then spatially and temporally overlapped on the silica/aqueous interface to generate the sum frequency light. SFG light from the sample was recollimated and filtered (Chroma, HQ 617/70 M) to remove the residual 800 nm light. It was then passed through a polarizer to select s or p-polarized SFG before being focused onto a spectrograph (Acton SP-2556 Imaging Spectrograph, grating: 1200 G/mm with 500-nm blaze wavelength), which was coupled with a thermoelectrically cooled (-75 °C), back-illuminated, charge coupled device camera (Acton PIXIS 100B CCD digital camera system, 1340 x 100 pixels, 20 μm x 20 μm pixel size, Princeton Instruments). Two polarization combinations were used in the SFG experiments, ssp (s-SFG, s-vis and p-IR) and pss (p-SFG, s-vis and s-IR).

Preparation of Silica Surface. IR grade silica hemispheres were obtained from Almaz Optics, NJ, USA. Prior to use, the hemisphere was cleaned by sonicating it in Milli-Q water (5 min), then in methanol (5 min) and finally in water (5 min) again, with copious rinses of Milli-Q water in between sonications. The hemisphere was then immersed in Piranha solution (3:1 mixture of H_2SO_4 and 30% H_2O_2, for an hour followed by thorough rinsing with Milli-Q water. The hemisphere was then sonicated in water for 5 minutes for a total of three times, with rinses of Milli-Q water in between sonications, The cleaned hemisphere was kept in the Millipore water until it was used for SFG experiments. Another hemisphere was cleaned in the same way as described above and coated with gold (thickness of 200 nm) through chemical vapor deposition to provide a standard for data normalization.

Preparation of Salt Solutions. Salt solutions (0.5 M) were prepared by dissolving salts in ultrapure deionized water (18.2 MΩ·cm, MilliQ-Plus ultrapure water purification system, Millipore). All the solutions were prepared by using the inorganic salts as obtained and without any further purification. The pH of the solutions was adjusted using the corresponding base (hydroxide of same alkali metal ions) or acid (same hydrochloric acid) solutions. The pH of all the solutions were measured with an Orion Versa Star, Star A, and Dual Star meters from Thermo Scientific (Orion, 8157UWMMD).

Materials. High purity salts, acids and bases were selected for preparation of the salt solutions NaCl (≥99.99%, Fisher Scientific) , NaOH (≥ 99.99%, Sigma-Aldrich) KCl (≥99.999%, Fisher Chemical), KOH (≥99.98%, Fisher Chemical), LiCl (≥99.99%, Sigma-Aldrich), LiOH (≥98%, Sigma-Aldrich), CsCl; (≥99.99%, Fisher Chemical), CsOH (≥99.9%, Fisher Chemical) and HCl (trace metal grade, Fisher Scientific) were used. Sulfuric acid (95.0-98.0%, Caledon Laboratories) and hydrogen peroxide were purchased from Sigma-Aldrich for Piranha cleaning. All materials were used without further purification. Ultrapure deionized water (18.2 MΩ) was used after deionization from a Milli-Q-Plus ultrapure water purification system (Millipore). All experiments were performed with freshly prepared solutions.

SFG Experiments. Prior to the start of each experiment, six reference SFG spectra were collected from a gold-coated IR grade silica surface covering the infrared region from 3000 to 3500 cm^{-1}, which includes the majority of the OH-stretching region of the water spectrum. The SFG spectra were adjusted by varying the incident IR wavelength so that the IR was centered at ~3000, 3100, 3200, 3300, 3400 and 3500 cm^{-1}. The gold-coated hemisphere was then replaced with a bare IR grade silica hemisphere and aligned using irises to make sure the reflected beam from the silica/water interface maintains the same alignment as the beam reflected from the gold surface. Similarly, six spectra at the same central wavenumbers were measured for the

silica/water interface. The six spectra from the silica/water interface were then summed to generate a single spectrum covering the broad water spectrum. The summed water spectrum was then normalized by dividing by the sum of the six gold reference spectra and finally smoothed to obtain the gold-normalized spectrum of interfacial water.[1,2] A freshly cleaned fused silica hemisphere (Almaz optics, 1 inch diameter, IR-grade SiO_2) was used for each SFG experiments. The hemisphere was placed on a custom-built Teflon cell so that the flat surface of the hemisphere was in contact with the aqueous phase. The silica/water interface was perpendicular to the surface of the laser table, and the aqueous phase was exposed so the pH could be routinely monitored and changed by adding solution from the top. Experiments for either a low pH or a high pH solution was performed for one cleaned hemisphere. First, SFG was measured for the silica/water interface with the Milli-Q water that has been equilibrated with air (~pH 5.6). The Milli-Q water was then replaced with ~10mL of the salt solution without pH adjustment (pH between 5-6 depending on the salt) and the interface was equilibrated for 30 min. After the equilibration time, a full spectrum was acquired. Aliquots of the corresponding acid or base solution with the same salt concentration (0.5 M) were added to adjust the pH by ~1 pH unit without altering salt concentration. After the addition of each aliquot, the solution was mixed by repeatedly removing and redispensing the solution with a glass pipet fit with a rubber bulb. At each new pH, the system was allowed to stand for ~3 min to reach equilibrium before the SFG spectrum was collected. For the high pH experiments, pH was adjusted in intervals of one pH unit until pH of the solution reached ~12.0. For the low pH experiments, pH was adjusted until pH of the solution reached ~ 2.0. Each experiment was performed a minimum of three times. The polarization combination ssp (s-SFG, s-vis and p-IR) was used, which is commonly used to measure interfacial water.[3-12] Additional experiments were performed using pss (p-SFG, s-vis and s-IR), which more selectively probes the 3400 cm^{-1} peak in the water spectrum.

II. Additional ssp-SFG data:

Raw, unsmoothed ssp spectra for pure water, 0.5 M CsCl, KCl, NaCl and LiCl are shown in Figure S1.

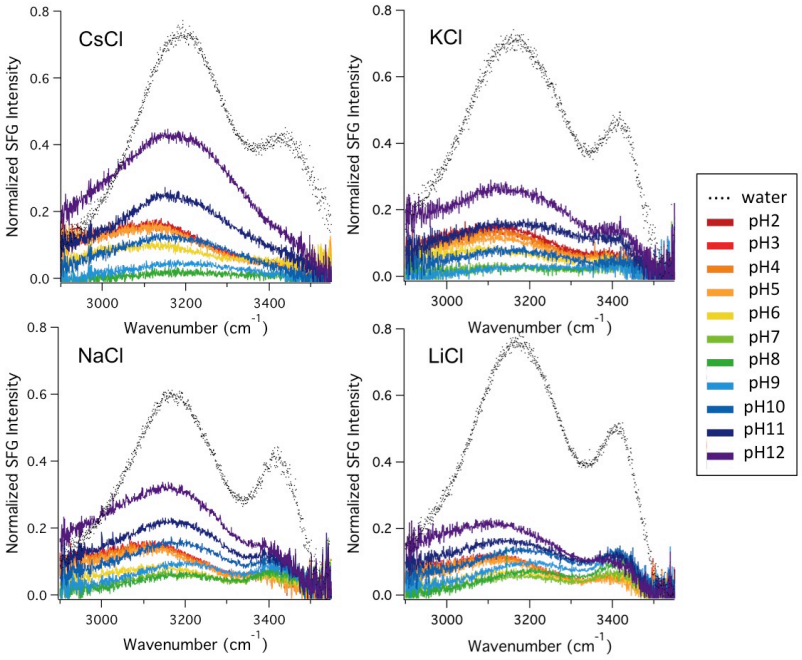

Figure S1. Unsmoothed, gold normalized SFG spectra for 0.5 M CsCl, KCl, NaCl and LiCl from pH 2-12. Also shown in Figure S1 are the spectra for pure water at pH 5.65 that was acquired prior to adding electrolyte.

Multiple replicate data sets were acquired for each salt and each pH range. The pH-dependent trends in gold-normalized SFG intensity were reproducible for all four salts, as shown in Figure S2.

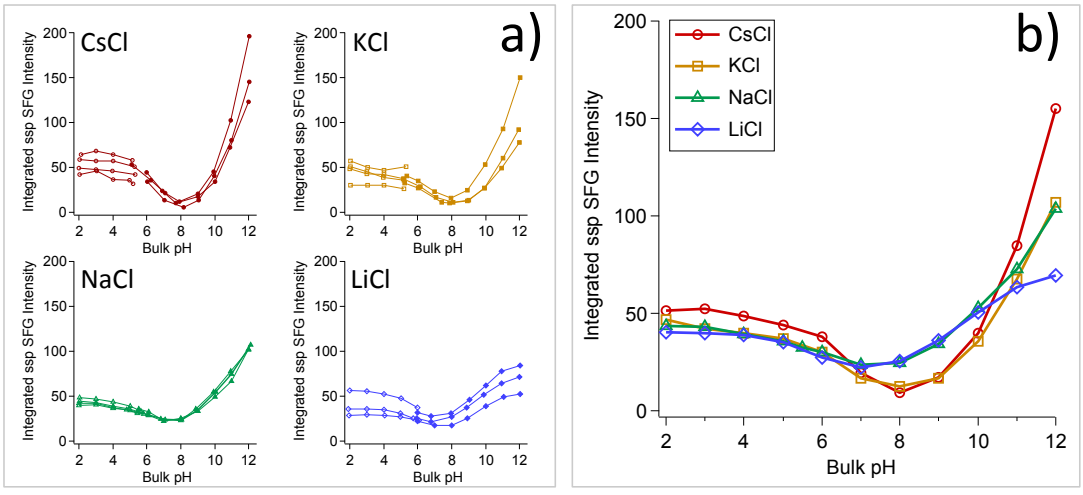

Figure S2. Individual integrated SFG intensity plots for replicate measurements of 0.5 M CsCl, KCl, NaCl and LiCl are shown in a) The mean of the replicate data at each pH point are shown for each salt in b).

In addition, the ratio of maximum integrated SFG intensity (occurring at pH 12) to minimum SFG intensity (pH 7-8) for the replicate data sets was reproducible, showing a clear Hofmeister trend (Figure S3).

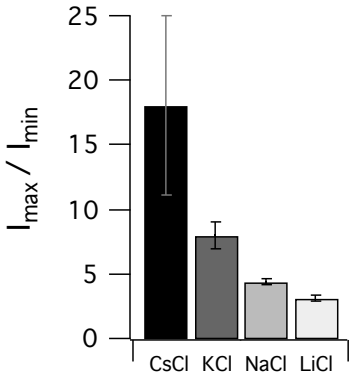

Figure S3. The ratio of maximum integrated SFG intensity (I_{max}) to minimum integrated SFG intensity (I_{min}) for 0.5 M CsCl, KCl, NaCl, LiCl.

III. SFG data acquired with the pss polarization combination at high pH

It has been shown that the pss polarization combination is most sensitive to the 3400 cm^{-1} peak compared to the 3200 cm^{-1} peak (Darlington et al, *J. Phys Chem C*, submitted for publication, 2017). We performed pss SFG experiments for 0.5 M CsCl and LiCl from pH 6-12 to observe whether the trends observed at high pH for the 3400 cm^{-1} peak in the ssp SFG spectrum were also consistent with those observed in the pss spectrum, the results of which are shown in Figure S4. In the reported ssp peak fitting results (Figure 3), distinct specific ion trends were observed in the 3400 cm^{-1} peak between LiCl and CsCl at high pH, where from pH 8 the peak amplitude for CsCl increased with increasing pH, while for Li the peak amplitude increased slightly from pH 8 to pH 10, but began to decrease again from pH 10 -12. This same trend was observed in the pss results shown in Figure S4c, where the 3400 cm^{-1} peak increased from pH 7-12 for CsCl yet increased from pH 6-10 and then decreased from 10 -12 for LiCl. The similarities in the 3400 cm^{-1} peak behavior as a function of pH for the two different polarization combinations indicate that the source of 3400 cm^{-1} peak in the ssp spectrum also contributes to the source of the 3400 cm^{-1} peak in the pss spectrum.

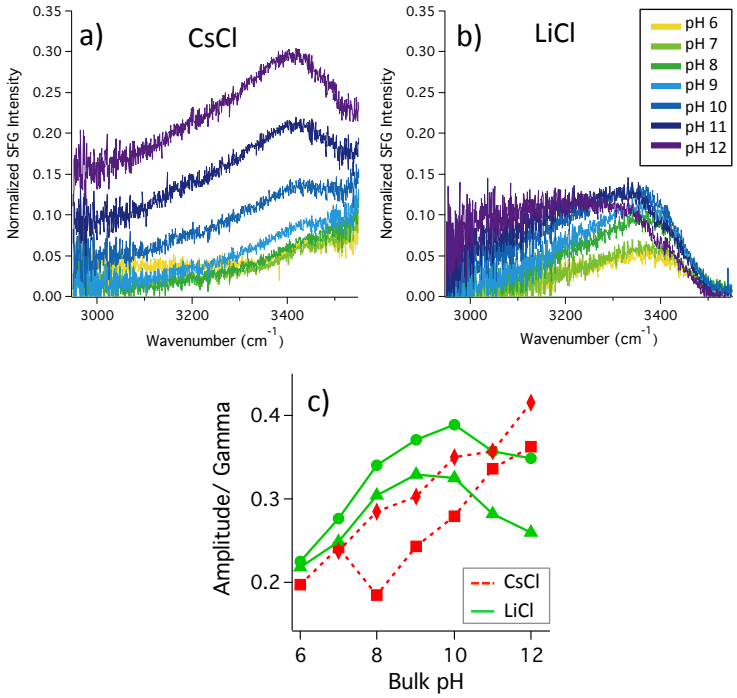

Figure S4. Unsmoothed, gold normalized pss SFG spectra are shown for 0.5 M LiCl a) and CsCl b) from pH 6 – 12. Peak fitting results of two replicate pss SFG data sets are also shown c).

IV. Predictions of the effect of ion hydration and charge reversal on SFG intensity

It is proposed that three peaks could be contributing to the broad peak observed at ~3200 in the ssp SFG spectrum 1) a positive peak at 3200 cm^{-1} that corresponds to waters in the diffuse layer aligned with their hydrogens pointing towards the surface by the *negative* Φ_{OH} 2) A negative red shifted peak from waters in the diffuse layer with their hydrogens pointed away from the surface aligned by a *positive* Φ_{OH} and 3) A negative red shifted peak corresponding to waters within the hydration layer of the cation or ordered by kosmotropic nature of the ion. As the pH decreases, the surface charge and $|\Phi_{OH}|$ decreases. As such, it is expected that the peak amplitude of peak 1 (A_{3200}) will decrease. When Φ_{OH} is negative, it is expected that peak 2 (A_{3150}) is zero, However, if Φ_{OH} becomes positive from overcharging, the magnitude of peak 2 (A_{3150}) should increase and be opposite in sign to peak 1, which is now zero. If peak 3 represents the hydration of the cation, it is expected to remain constant for as long as the ion is present at the surface and be opposite in sign to peak 1 as the waters will be oriented with their hydrogens pointing towards the cation. This peak is also expected to be red-shifted from waters in the diffuse layer, with a frequency ~ 3150 cm^{-1}.[13] Figure S4 shows the predicted shape and intensity trend for these three predicted interfering Lorentzian peaks. Similar to the experimental SFG spectra as a function of pH, as the intensity of A_{3200} decreases, the predicted SFG intensity decreases. However, a minimum in predicted intensity is observed when A_{3200} equals the amplitude of the constant hydration peak at 3150 cm^{-1} (shown in red). In addition, the intensity of the signal at the minimum is greater when the amplitude of the constant hydration peak is greater. As the amplitude of the hydration peak

becomes larger in amplitude than A_{3200}, the predicted signal begins to increase again, but red shifted. The appearance of peak 2, the red-shifted negative peak as a result of positive Φ_{OH} at low pH, also contributes to the increase in the red shifted peak.

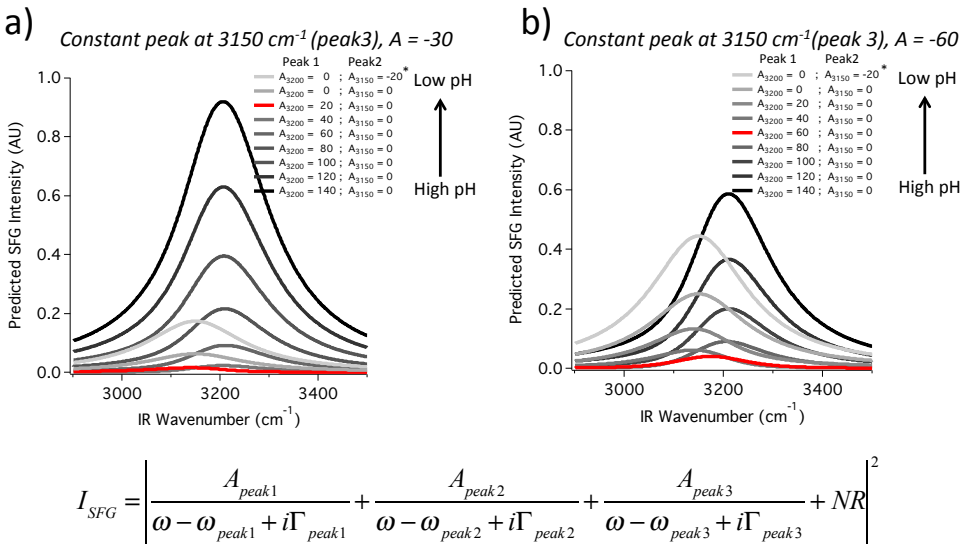

$$I_{SFG} = \left| \frac{A_{peak1}}{\omega - \omega_{peak1} + i\Gamma_{peak1}} + \frac{A_{peak2}}{\omega - \omega_{peak2} + i\Gamma_{peak2}} + \frac{A_{peak3}}{\omega - \omega_{peak3} + i\Gamma_{peak3}} + NR \right|^2$$

Figure S5. Predicted SFG intensity for 3 interfering peaks with different amplitudes (Γ = 120 cm^{-1} for all peaks) .The peak amplitude of the constant peak at 3150 cm^{-1} is a) -30 and b) -60. The spectrum where the minimum in predicted SFG intensity occurs is shown in red. * indicates a where overcharging of the EDL occurs. The equation used to simulated the interfering peaks is also shown.

V. Peak Fitting

Spectral data were fit to the following equation:

$$I_{SFG} = \left| \frac{A_{3200\,peak}}{\omega_{IR} - \omega_{3200\,peak} + i\Gamma} + \frac{A_{3400\,peak}}{\omega_{IR} - \omega_{3400\,peak} + i\Gamma} + NR \right|^2 .$$

Where, A is peak amplitude, ω is peak frequency and Γ is the linewidth. For all fits the non-resonant term (NR) was constrained to be negative, resulting in positive values for both A_{3200} and A_{3400}. However, in this work we suggest that at low pH water may be flipping in the diffuse layer (3200 cm^{-1} peak) but not flipping in the Stern layer (3400 cm^{-1} peak), which would manifest in oppositely signed A_{3200} and A_{3400} . However, if the NR term is constrained to be positive, equivalent fits can be obtained that result in a negatively signed A_{3200} and positively signed A_{3400} . This creates ambiguity in the signage of A_{3200} and NR, but nevertheless the overall trends in |A/Γ| are similar for both fitting scenarios: 1) negative NR and positive A_{3200} or 2) positive NR and negative A_{3200}.

REFERENCES:

(1) Azam, M. S.; Weeraman, C. N.; Gibbs-Davis, J. M. Halide-Induced Cooperative Acid–Base Behavior at a Negatively Charged Interface. *J. Phys. Chem. C* **2013**, *117*, 8840.

(2) Azam, M. S.; Darlington, A. M.; Gibbs-Davis, J. M. The Influence of Concentration on Specific Ion Effects at the Silica/Water Interface. *J. Phys-Condens. Mat.* **2014**, *26*, 244107.

(3) Covert, P. A.; Hore, D. K. Geochemical Insight from Nonlinear Optical Studies of Mineral–Water Interfaces. *Annu. Rev. Phys. Chem.* **2016**, *67*, 233.

(4) Dewan, S.; Mohsen S. Yeganeh; Borguet, E. Experimental Correlation Between Interfacial Water Structure and Mineral Reactivity. *J. Phys. Chem. Lett.* **2013**, *4*, 1977.

(5) Eisenthal, K. B. Liquid interfaces probed by second-harmonic and sum-frequency spectroscopy. *Chem. Rev.* **1996**, *96*, 1343.

(6) Jena, K. C.; Hore, D. K. Variation of Ionic Strength Reveals the Interfacial Water Structure at a Charged Mineral Surface. *J. Phys. Chem. C.* **2009**, *113*, 15364.

(7) Kim, J.; Cremer, P. S. IR−Visible SFG Investigations of Interfacial Water Structure upon Polyelectrolyte Adsorption at the Solid/Liquid Interface. *J. Am. Chem. Soc.* **2000**, *122*, 12371.

(8) Myalitsin, A.; Urashima, S.-h.; Nihonyanagi, S.; Yamaguchi, S.; Tahara, T. Water Structure at the Buried Silica/Aqueous Interface Studied by Heterodyne-Detected Vibrational Sum-Frequency Generation. *J. Phys. Chem. C.* **2016**, *120*, 9357.

(9) Nihonyanagi, S.; Yamaguchi, S.; Tahara, T. Direct Evidence for Orientational Flip-flop of Water Molecules at Charged Interfaces: A Heterodyne-detected Vibrational Sum Frequency Generation Study. *J. Chem. Phys.* **2009**, *130*, 204704.

(10) Ong, S.; Zhao, X.; Eisenthal, K. B. Polarization of Water Molecules at a Charged Interface: Second Harmonic Studies of the Silica/Water Interface. *Chem. Phys. Lett.* **1992**, *191*, 327.

(11) Ostroverkhov, V.; Waychunas, G. A.; Shen, Y. R. Vibrational spectra of water at water/α-quartz (0 0 0 1) interface. *Chem. Phys. Lett.* **2004**, *386*, 144.

(12) Yang, Z.; Li, Q.; Chou, K. C. Structures of Water Molecules at the Interfaces of Aqueous Salt Solutions and Silica: Cation Effects. *J. Phys. Chem. C* **2009**, *113*, 8201.

(13) Schultz, Z. D.; Shaw, S. K.; Gewirth, A. A. Potential Dependent Organization of Water at the Electrified Metal−Liquid Interface. *J. Am. Chem. Soc.* **2005**, *127*, 15916.